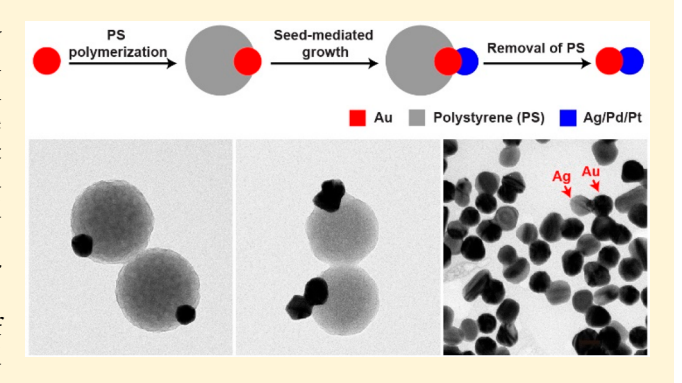
General Approach to the Synthesis of Heterodimers of Metal Nanoparticles through Site-Selected Protection and Growth

Jichuan Qiu,^{†,‡} Minghao Xie,[§] Zhiheng Lyu,[§] Kyle D. Gilroy,[†] Hong Liu,[‡] and Younan Xia*,^{†,§}

Supporting Information

ABSTRACT: Heterodimers of metal nanoparticles are widely sought for applications in photonics, sensing, and catalysis. In this work, we demonstrate a general approach to the fabrication of heterodimers of metal nanoparticles by leveraging the concept of site-selected growth under the protection of an inert material. When styrene is polymerized in the presence of Au nanoparticles, the resultant polystyrene (PS) can be controlled to grow from only one portion of the surface of a nanoparticle. Free of PS, the remaining portion can serve as an active site for the heterogeneous nucleation and growth of the second metal. After dissolving the PS component, we obtain heterodimers of metal nanoparticles with tunable elemental compositions and controllable physical dimensions. The contact area between the



two metals can also be maneuvered by adjusting the concentration of divinylbenzene used for copolymerization with styrene. Using this method, we have prepared Au-Ag, Au-Pd, and Au-Pt heterodimers and further investigated their plasmonic properties. The capability of this approach should be extendible to the fabrication of heterodimers with a broader range of compositions and properties.

KEYWORDS: Heterodimers, bimetallic nanoparticles, seed-mediated growth, symmetry breaking, plasmonics

here is an ever-growing interest in the synthesis of dimers of metal nanoparticles because of their unique plasmonic, photonic, catalytic, and magnetic properties. ^{1–3} Homodimers consisting of Ag and Au nanoparticles, for example, have been demonstrated with greater surface-enhanced Raman scattering (SERS) activity than individual Ag or Au nanoparticles.^{4,5} As a result of the significant enhancement of the local electric field in the gap region of a dimer, it is even feasible to detect analytes down to the single-molecule level. Heterodimers made of two different metals (e.g., Au–Ag, Au–Pd, or Au–Pt) have been demonstrated with optical properties distinctive from the homodimers because of asymmetric electromagnetic coupling. 7-9 To this end, both bonding and antibonding plasmon modes as well as enhanced Fano resonance have been observed in Au-Ag heterodimers. 10,11 In addition, heterodimers support electron transfer between the two metals with distinct work functions, leading to catalytic properties superior to their counterparts made of the same metal. 12-14

As a commonly used strategy, one can force colloidal nanoparticles to dimerize through the introduction of a salt at a high concentration or by modifying the surface of the nanoparticles with molecular linkers containing oppositely charged or cross-linkable groups. 15-17 Unfortunately, these methods generally act in an uncontrollable fashion, and the

products are often plagued by aggregates composed of more than two nanoparticles. In addition, it is difficult to remove the molecular linkers between the nanoparticles, and the presence of linkers may prevent electronic coupling between the two nanoparticles and thus compromise the catalytic or plasmonic properties. The site-selected growth of a second metal on the surface of a pre-existing metal nanocrystal offers an effective route to the formation of heterodimers of metal nanoparticles with direct contact. ^{18,19} To obtain a dimeric Janus structure, the reaction kinetics, ^{20–23} the capping agent on the surface of the seed,^{24–27} as well as the lattice mismatch between the seed metal and deposited metal²⁸⁻³⁰ all need to be carefully optimized. This approach, although successful to different levels depending on the metals involved, is limited to several metals only, making it difficult to explore heterodimers with a broad range of elemental compositions. Asymmetrically masking the surface of a seed with an inert material such as SiO₂ or Fe₃O₄, followed by seed-mediated growth and then removal of the inert mask, offers an alternative route to the facile production of heterodimers. 16,31-36 However, the

Received: August 1, 2019 Published: August 26, 2019

[†]The Wallace H. Coulter Department of Biomedical Engineering, Georgia Institute of Technology and Emory University, Atlanta, Georgia 30332, United States

[‡]State Key Laboratory of Crystal Materials, Shandong University, Jinan, Shandong 250100, P. R. China

[§]School of Chemistry and Biochemistry, Georgia Institute of Technology, Atlanta, Georgia 30332, United States

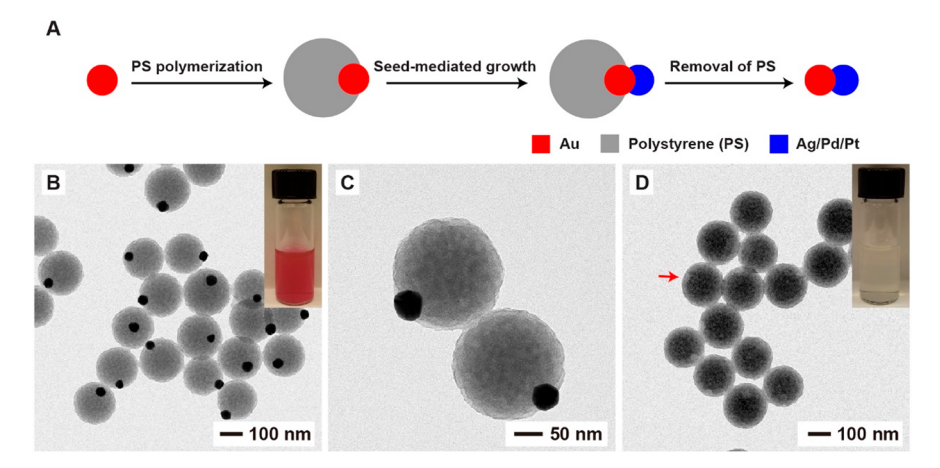


Figure 1. (A) Schematic illustration showing the synthesis of heterodimers of metal nanoparticles through site-selected protection and growth. (B,C) TEM images, at two different magnifications, of the PS—Au Janus particles. (D) TEM images of the PS—Au Janus particles after the Au component had been etched away with KI/I₂. The insets in panels B and D show digital photographs of the aqueous suspensions of PS—Au Janus particles before and after Au etching. The red arrow in panel D indicates the hole left behind after the removal of Au nanoparticle by etching.

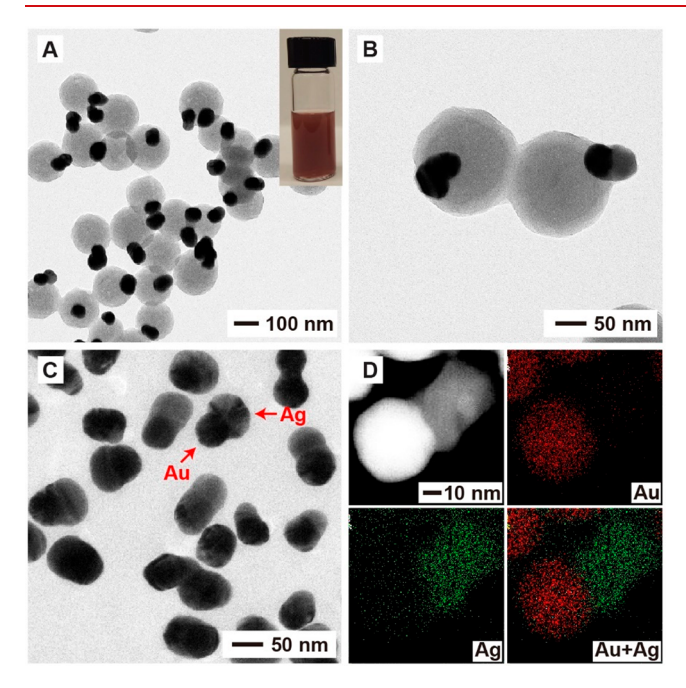


Figure 2. (A,B) TEM images, at two different magnifications, of the PS-Au-Ag particles that were prepared at a styrene to DVB ratio of 200:1 (v/v). (C) TEM image of the Au-Ag dimers after selective dissolution of PS from the sample in panel A using THF. (D) HAADF-STEM image together with the EDX mapping of an individual Au-Ag dimer from the sample in panel C. The inset in panel A shows a digital micrograph recorded from an aqueous suspension of the corresponding particles.

asymmetric modification process often requires a dedicated control over multiple parameters, making it less appealing for large-scale production. Taken together, there is still a critical need to develop a simple and general method for the synthesis of heterodimers of metal nanoparticles.

In a prior study, we demonstrated a facile method for the synthesis of polymer—metal hybrid colloidal particles with a Janus structure.^{37,38} During the polymerization and deposition of PS, symmetry reduction occurred naturally, resulting in the formation of a partially protected surface for the Au nanoparticle. Here we demonstrate that such Janus particles

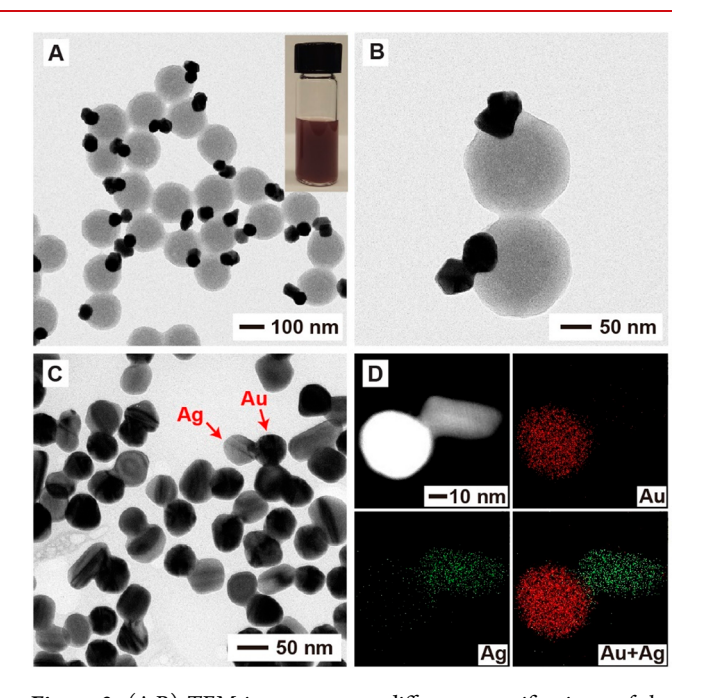


Figure 3. (A,B) TEM images, at two different magnifications, of the PS-Au-Ag particles that were prepared at a styrene to DVB ratio of $100:1\ (v/v)$. (C) TEM image of Au-Ag dimers after the selective dissolution of PS from the sample in panel A with THF. (D) HAADF-STEM image and the corresponding EDX mapping of a Au-Ag dimer from the sample in panel C. The inset in panel A shows a digital micrograph recorded from an aqueous suspension of the corresponding particles.

can be used to fabricate heterodimers of metal nanoparticles by leveraging the partial protection of the metal surface by PS. As shown in Figure 1A, the partially protected Au nanoparticle can serve as a seed for the site-selected growth of another metal such as Ag, Pd, or Pt for the generation of a PS-Au-M (M = Ag, Pd, or Pt) colloidal particle in the dimeric configuration. In this new approach, there is no need to strictly control the experimental parameters such as the reduction kinetics, the type of capping agent, and the type of precursor. When the PS component is dissolved, we obtain a Au-M heterodimer with controllable dimensions for both

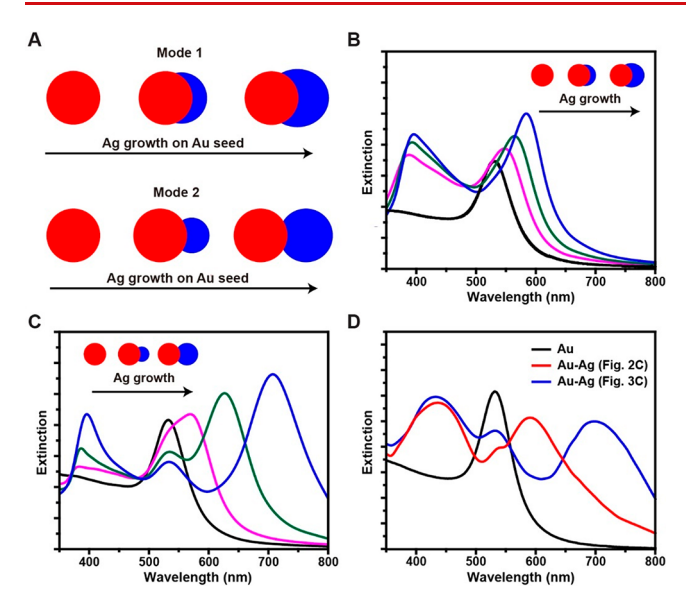


Figure 4. (A) Schematic illustration showing the growth of Ag from one side of a Au nanoparticle to generate Au–Ag dimers with different areas of contact. (B,C) Optical spectra calculated for the Au–Ag dimers obtained through (B) mode 1 and (C) mode 2, respectively. (D) UV–vis extinction spectra recorded from aqueous suspensions of the Au nanoparticles and the Au–Ag dimers shown in Figures 2C and 3C, respectively.

components and a well-defined contact area between them. Because only solution-phase protocols are involved, the syntheses of both PS—Au and PS—Au—M colloidal particles can be potentially scaled up for high-volume production.

The PS-Au Janus particles could be routinely produced by controlling the delay between the initiation of PS polymerization and the introduction of citrate-covered Au nanoparticles (Figure S1). Figure 1B,C shows transmission electron microscopy (TEM) images of the as-obtained PS-Au particles, in which the styrene to divinylbenzene (DVB) ratio was set to 200:1. The PS-Au particles were uniform in size, with an average diameter of 190 nm. Each particle contained only one Au nanoparticle positioned on the surface, with a purity approaching 100%. The aqueous suspension of the particles showed a ruby red color (inset in Figure 1B), confirming the absence of dimerization or aggregation for the Au nanoparticles. The particles could be easily dispersed in an aqueous medium due to the electrostatic repulsions between the 4styrenesulfonic acid groups on the PS surface. The TEM image at a higher magnification (Figure 1C) indicates that the Au nanoparticle was partially embedded in the PS component. As demonstrated in our prior studies, the PS grew from only one side of a citrate-covered Au nanoparticle during the polymerization process.³⁷ To confirm that the Au nanoparticle was indeed partially embedded in PS, we exposed the assynthesized PS-Au Janus particles to an aqueous Au etchant containing KI and I2. After 5 min, the suspension became colorless (inset in Figure 1D), indicating the dissolution of all the Au nanoparticles. The TEM image in Figure 1D confirms that the Au nanoparticles have been etched away from the PS-Au particles, creating a dimple on the surface of the particle. Considering that PS is largely impermeable to the KI/I₂ etchant, the successful etching of Au nanoparticles by KI/I₂ suggests that the Au nanoparticle was only partially covered by PS. This assertion is further supported by the observation that when heated to 95 °C for 30 min, the Au

nanoparticles could not be etched away by the KI/I_2 etchant, as indicated by the preservation of the red color (Figure S2). In this case, the migration of PS at a temperature slightly above its glass-transition temperature (93 °C) could cover and protect the entire Au surface with PS. Collectively, these results confirm that the Au nanoparticle in each PS—Au Janus particle was only partially coated by PS.

To leverage the unique structure of PS-Au Janus particles, we applied them as seeds for the site-selected nucleation and growth of another metal such as Ag for the production of Au-Ag heterodimers. In a typical synthesis, the PS-Au particles were added to an aqueous solution containing poly-(vinylpyrrolidone) (PVP) and CF₃COOAg and incubated for 30 min, followed by the injection of ascorbic acid (AA) as a reducing agent. Within 10 min, the suspension gradually changed color from ruby red to brown (inset in Figure 2A), implying the formation of Au-Ag heteronanostructures. The TEM image in Figure 2A validates the formation of a Ag nanoparticle on each Au nanoparticle, generating PS-Au-Ag particles with a nonconcentric structure. The high affinity of Ag toward Au made it easier for the Ag atoms to nucleate and grow from the exposed region on a Au nanoparticle rather than the PS-covered region (Figure 2B). In this way, the growth of Ag nanoparticle occurred asymmetrically along one side of the Au nanoparticle. We obtained Au-Ag heterodimers by selectively removing the PS component in tetrahydrofuran (THF) in the presence of PVP, a colloidal stabilizer that could prevent the Au-Ag dimers from aggregation. Given the intrinsic lower contrast of Ag relative to Au under the electron beam, the heterostructure could be easily identified in the TEM image (Figure 2C). Each Au-Ag dimer was composed of a Au and a Ag nanoparticle, whose average diameters were about 55 and 58 nm, respectively, whereas the diameter of the contact area between the Au and Ag nanoparticles was 48 nm on average. We also characterized the heterostructure by highangle annular dark-field scanning transmission electron microscopy (HAADF-STEM) and energy-dispersive X-ray (EDX) spectroscopy mapping analyses. From the HAADF-STEM image in Figure 2D, it can be clearly seen that the bright Au and dark Ag were distributed at two opposite sides of the dimer, with a clear boundary between them. The EDX mapping confirms the spatial separation between Au (red) and Ag (green), further confirming the well-defined heterodimer structure.

As demonstrated in the literature, the optical and catalytic properties of the dimers are strongly correlated with the spatial distribution of the two metals.^{25,39} In our system, the increase in DVB used for PS polymerization would result in the formation of PS over a larger area on the Au nanoparticle. This trend can be used to tune the spatial distribution of the Au and Ag nanoparticles in the dimers. When PS-Au particles were prepared at a styrene to DVB ratio of 100:1, a larger portion of the Au nanoparticle would be embedded in the PS bead (Figure S3). We could still grow a Ag nanoparticle from the exposed Au region on the PS-Au particle, producing a black brown colloidal suspension (inset in Figure 3A). The TEM images in Figure 3A,B indicate that the contact area between the Ag and Au components in these particles was much smaller than that in the PS-Au-Ag particles shown in Figure 2A. After the removal of PS with THF, Au-Ag heterodimers composed of 55 nm Au and 56 nm Ag nanoparticles were obtained (Figure 3C). The average diameter of the contact area was reduced from 48 to 29 nm when compared with the

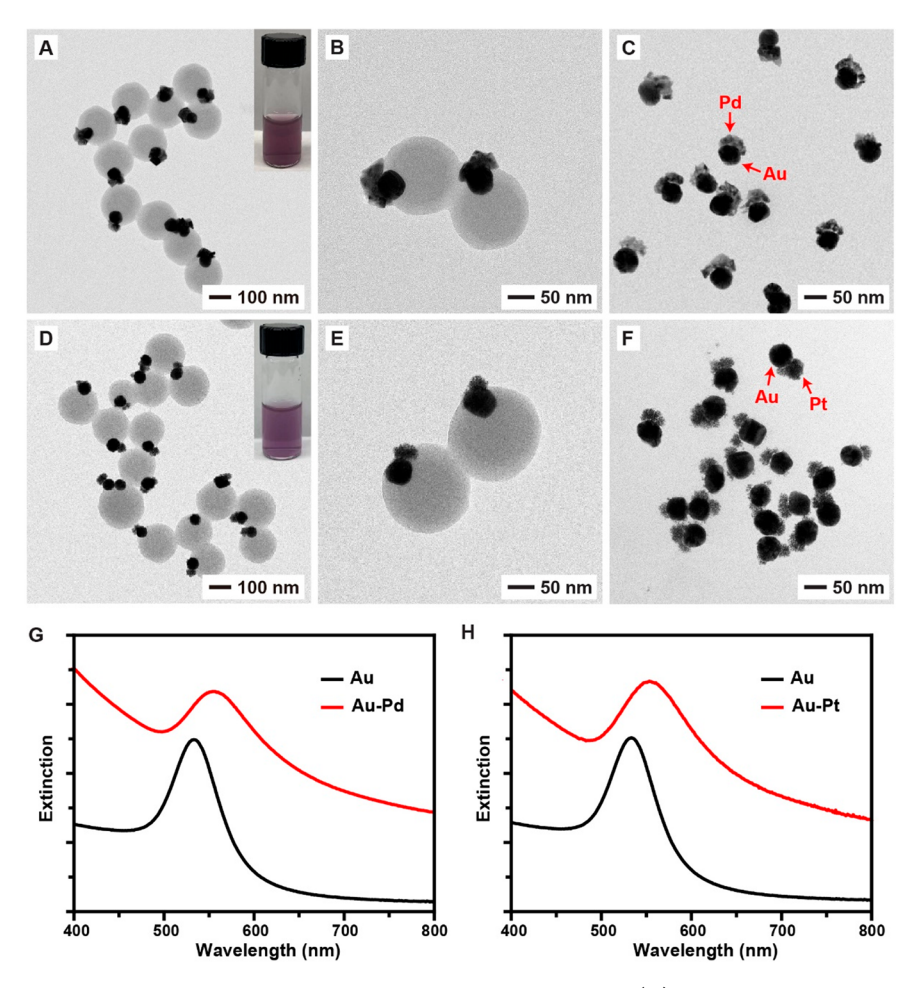


Figure 5. (A,B) TEM images, at two different magnifications, of the PS-Au-Pd particles. (C) TEM image of Au-Pd dimers after the selective dissolution of PS from the sample in panel A with THF. (D,E) TEM images, at two different magnifications, of the PS-Au-Pt particles. (F) TEM image of Au-Pt dimers after the selective removal of PS from the sample in panel D with THF. UV-vis extinction spectra recorded from aqueous suspensions of the (G) Au-Pd dimers and (H) Au-Pt dimers. The insets in panels A and D show digital micrographs recorded from aqueous suspensions of the corresponding colloidal particles, respectively.

Au—Ag dimers in Figure 2C. The HAADF-STEM and EDX mapping data in Figure 3D further confirm the reduction in contact area between the Au and Ag components.

To investigate the optical properties of the Au-Ag dimers with different spatial distributions of Ag and Au, we first established two simulation models regarding the heterogeneous growth of Ag on Au seeds differing in contact area (Figure 4A). Specifically, the Au nanoparticle serving as the seed was set to 55 nm in diameter, and then Ag was gradually deposited onto one side of the seed with contact areas of 48 (mode 1) and 29 nm (mode 2) in diameter, respectively. Figure 4B shows the optical spectra calculated for the Au-Ag dimers during the gradual deposition of Ag onto Au in mode 1. Upon the deposition of Ag, the extinction peak of Ag at 400 nm emerged and was red-shifted gradually. In parallel, the peak of Au was also gradually red-shifted from the initial position at 530 nm due to the electromagnetic coupling to the Ag nanoparticle. When Ag was gradually grown from Au in mode 2, similarly, the extinction peak of Ag initially emerged at 400 nm and was then red-shifted with the increase in size for Ag (Figure 4C). Differently, the peak around 530 nm, representative of Au, still existed, whereas a new peak appeared at 580 nm and was red-shifted to 706 nm with the growth of Ag. This trend could be attributed to the electromagnetic

coupling between the Ag and Au nanoparticles in a fashion different from what was described in mode 1. These simulation results were consistent with experimental observations. Figure 4D shows the UV-vis spectra of Au seeds and Au-Ag dimers prepared with different contact areas in correspondence to the products shown in Figures 2C and 3C, respectively. The Au-Ag dimers in Figure 2C were featured with two extinction peaks located at 421 (Ag) and 592 nm (coupling between Au and Ag), with a negligible peak at 531 nm (Au). For the Au-Ag dimers with a smaller contact area (Figure 3C), there were three peaks at 417, 531, and 698 nm, which were attributed to Ag nanoparticles, Au nanoparticles, and the electromagnetic coupling between Au and Ag nanoparticles, respectively. These results demonstrate that the electromagnetic coupling between Au and Ag in the Au-Ag dimers could greatly change their optical properties, in a manner dependent on the contact area.

We also extended this strategy to produce other kinds of heterodimers of metal nanoparticles. In one example, PS-Au Janus particles were used as seeds and dispersed in an aqueous solution containing hexadecyltrimethylammonium bromide (CTAB) and H₂PdCl₄. After the addition of AA, the suspension gradually turned from ruby red to dark brown (inset in Figure 5A). The TEM image in Figure 5A shows that Pd was selectively grown from the unprotected region on Au

nanoparticles, generating PS-Au-Pd particles. Similar to Ag, the deposition of Pd occurred solely at the exposed region on each Au nanoparticle (Figure 5B). After the dissolution of PS in THF, we obtained Au-Pd dimers (Figure 5C). When the precursor was switched to K₂PtCl₄, we obtained PS-Au-Pt particles (Figure 5D). Again, small Pt nanoparticles were deposited only on the exposed region on the Au nanoparticle (Figure 5E). In the same way, Au-Pt dimers (Figure 5F) were obtained after the removal of PS. The UV-vis spectra suggest that the extinction peaks of the Au-Pd dimers (Figure 5G) and Au-Pt dimers (Figure 5H) were red-shifted and became broader relative to the pristine Au nanoparticles because of the electromagnetic coupling between Au and Pd (Pt), which was consistent with a previous report on the Au-Pd dimers.²⁷

This approach to the synthesis of heterodimers of metal nanoparticles based on PS-Au Janus particles can also be extended to metals other than Ag, Pd, and Pt as long as they can nucleate and grow from the Au surface. For example, homodimers of Au nanoparticles could also be obtained by switching to a Au-based precursor for the second metal (Figure S4). In addition, we have demonstrated that PS could also anisotropically grow on other types of metal nanoparticles, such as those made of Pd and Pt, resulting in Pd or Pt nanoparticles partially encapsulated and protected by PS.38 This will allow us to further expand the diversity of metals contained in the heterodimers. We believe that this strategy, in which PS-metal Janus particles serve as a selectively protected seed for the nucleation and growth of another metal, could be applied to different combinations of essentially all noble metals. In general, this approach has no strict requirement for the reaction kinetics, capping agent, and level of lattice mismatch between the seed and the metal deposited.

In summary, we have demonstrated a facile and general method for the synthesis of heterodimers of metal nanoparticles. Starting with PS-Au Janus particles, we have successfully prepared Au-Ag, Au-Pd, and Au-Pt heterodimers through the site-selected nucleation and growth of the second metal from the bare region on Au nanoparticles unprotected by PS. By controlling the area exposed on the surface of the Au nanoparticle through the adjustment of the DVB concentration, we were able to tune the contact area between the two metals in a heterodimer, which could be further used to tailor the optical properties of the dimers. We believe that this method could be extended to other combinations of metals, opening an opportunity to explore a broad range of heterodimers with different elemental distributions and physical dimensions.

ASSOCIATED CONTENT

S Supporting Information

The Supporting Information is available free of charge on the ACS Publications website at DOI: 10.1021/acs.nanolett.9b03167.

Experimental details are provided, together with TEM images of the Au nanoparticles, the PS-Au Janus particles after heating, the PS-Au Janus particles prepared under different experimental conditions, and PS-Au-Au particles (PDF)

AUTHOR INFORMATION

Corresponding Author

*E-mail: younan.xia@bme.gatech.edu.

ORCID ®

Jichuan Qiu: 0000-0002-9993-8220 Minghao Xie: 0000-0003-3781-5118 Zhiheng Lyu: 0000-0002-1343-4057 Kyle D. Gilroy: 0000-0002-3153-8060 Hong Liu: 0000-0003-1640-9620 Younan Xia: 0000-0003-2431-7048

Notes

The authors declare no competing financial interest.

ACKNOWLEDGMENTS

This work was partially supported by a grant from the NSF (MSN-1804970) and startup funds from the Georgia Institute of Technology. As a visiting graduate student from Shandong University, J.Q. was also partially supported by a fellowship from the China Scholarship Council.

REFERENCES

- (1) Jiang, N.; Zhuo, X.; Wang, J. Chem. Rev. 2018, 118, 3054-3099.
- (2) Zhang, C.; Zhao, H.; Zhou, L.; Schlather, A. E.; Dong, L.; McClain, M. J.; Swearer, D. F.; Nordlander, P.; Halas, N. J. *Nano Lett.* **2016**, *16*, 6677–6682.
- (3) Sun, M.; Xu, L.; Bahng, J. H.; Kuang, H.; Alben, S.; Kotov, N. A.; Xu, C. Nat. Commun. 2017, 8, 1847.
- (4) Chen, G.; Wang, Y.; Yang, M.; Xu, J.; Goh, S. J.; Pan, M.; Chen, H. J. Am. Chem. Soc. **2010**, 132, 3644–3645.
- (5) Li, W.; Camargo, P. H.; Lu, X.; Xia, Y. Nano Lett. 2009, 9, 485-490.
- (6) Camden, J. P.; Dieringer, J. A.; Wang, Y.; Masiello, D. J.; Marks, L. D.; Schatz, G. C.; Van Duyne, R. P. J. Am. Chem. Soc. 2008, 130, 12616–12617.
- (7) Sun, Y.; Foley, J. J., IV; Peng, S.; Li, Z.; Gray, S. K. Nano Lett. **2013**, 13, 3958–3964.
- (8) Brown, L. V.; Sobhani, H.; Lassiter, J. B.; Nordlander, P.; Halas, N. J. *ACS Nano* **2010**, *4*, 819–832.
- (9) Tumkur, T.; Yang, X.; Zhang, C.; Yang, J.; Zhang, Y.; Naik, G. V.; Nordlander, P.; Halas, N. J. *Nano Lett.* **2018**, *18*, 2040–2046.
- (10) Peña-Rodríguez, O.; Pal, U.; Campoy-Quiles, M.; Rodríguez-Fernández, L.; Garriga, M.; Alonso, M. *J. Phys. Chem. C* **2011**, *115*, 6410–6414.
- (11) Sheikholeslami, S.; Jun, Y.-w.; Jain, P. K.; Alivisatos, A. P. *Nano Lett.* **2010**, *10*, 2655–2660.
- (12) Hu, Y.; Liu, Y.; Li, Z.; Sun, Y. Adv. Funct. Mater. 2014, 24, 2828–2836.
- (13) Zheng, Z.; Li, H.; Shen, Y.; Cao, R. Chem. Eur. J. 2011, 17, 8440-8444.
- (14) Li, W.; Camargo, P. H.; Au, L.; Zhang, Q.; Rycenga, M.; Xia, Y. *Angew. Chem., Int. Ed.* **2010**, 49, 164–168.
- (15) Sardar, R.; Heap, T. B.; Shumaker-Parry, J. S. J. Am. Chem. Soc. 2007, 129, 5356-5357.
- (16) Gschneidtner, T. A.; Fernandez, Y. A. D.; Syrenova, S.; Westerlund, F.; Langhammer, C.; Moth-Poulsen, K. *Langmuir* **2014**, 30, 3041–3050.
- (17) Chen, G.; Wang, Y.; Tan, L. H.; Yang, M.; Tan, L. S.; Chen, Y.; Chen, H. J. Am. Chem. Soc. **2009**, 131, 4218–4219.
- (18) Gilroy, K. D.; Ruditskiy, A.; Peng, H. C.; Qin, D.; Xia, Y. Chem. Rev. 2016, 116, 10414–10472.
- (19) Xia, Y.; Gilroy, K. D.; Peng, H. C.; Xia, X. Angew. Chem., Int. Ed. **2017**, 56, 60–95.
- (20) Zeng, J.; Zhu, C.; Tao, J.; Jin, M.; Zhang, H.; Li, Z. Y.; Zhu, Y.; Xia, Y. Angew. Chem., Int. Ed. 2012, 51, 2354–2358.
- (21) Zhu, C.; Zeng, J.; Tao, J.; Johnson, M. C.; Schmidt-Krey, I.; Blubaugh, L.; Zhu, Y.; Gu, Z.; Xia, Y. J. Am. Chem. Soc. 2012, 134, 15822–15831.
- (22) Lim, B.; Kobayashi, H.; Yu, T.; Wang, J.; Kim, M. J.; Li, Z.-Y.; Rycenga, M.; Xia, Y. J. Am. Chem. Soc. **2010**, 132, 2506–2507.

(23) Gilroy, K. D.; Peng, H. C.; Yang, X.; Ruditskiy, A.; Xia, Y. Chem. Commun. 2017, 53, 4530-4541.

- (24) Lee, S. U.; Hong, J. W.; Choi, S. I.; Han, S. W. J. Am. Chem. Soc. **2014**, 136, 5221–5224.
- (25) Feng, Y.; He, J.; Wang, H.; Tay, Y. Y.; Sun, H.; Zhu, L.; Chen, H. J. Am. Chem. Soc. 2012, 134, 2004–2007.
- (26) Feng, Y.; Wang, Y.; He, J.; Song, X.; Tay, Y. Y.; Hng, H. H.; Ling, X. Y.; Chen, H. J. Am. Chem. Soc. 2015, 137, 7624-7627.
- (27) Liu, B.; Thanneeru, S.; Lopes, A.; Jin, L.; McCabe, M.; He, J. Small **2017**, 13, 1700091.
- (28) Jin, M.; Zhang, H.; Wang, J.; Zhong, X.; Lu, N.; Li, Z.; Xie, Z.; Kim, M. J.; Xia, Y. ACS Nano **2012**, 6, 2566–2573.
- (29) Wang, Z.; Chen, Z.; Zhang, H.; Zhang, Z.; Wu, H.; Jin, M.; Wu, C.; Yang, D.; Yin, Y. ACS Nano 2015, 9, 3307-3313.
- (30) Habas, S. E.; Lee, H.; Radmilovic, V.; Somorjai, G. A.; Yang, P. *Nat. Mater.* **2007**, *6*, 692–697.
- (31) Hu, Y.; Sun, Y. J. Am. Chem. Soc. 2013, 135, 2213-2221.
- (32) Chen, T.; Chen, G.; Xing, S.; Wu, T.; Chen, H. Chem. Mater. 2010, 22, 3826-3828.
- (33) Crane, C. C.; Tao, J.; Wang, F.; Zhu, Y.; Chen, J. J. Phys. Chem. C 2014, 118, 28134–28142.
- (34) Buck, M. R.; Bondi, J. F.; Schaak, R. E. Nat. Chem. 2012, 4, 37–44.
- (35) Read, C. G.; Gordon, T. R.; Hodges, J. M.; Schaak, R. E. J. Am. Chem. Soc. 2015, 137, 12514–12517.
- (36) Feng, J.; Yang, F.; Wang, X.; Lyu, F.; Li, Z.; Yin, Y. Adv. Mater. **2019**, 31, 1900789.
- (37) Ohnuma, A.; Cho, E. C.; Camargo, P. H.; Au, L.; Ohtani, B.; Xia, Y. J. Am. Chem. Soc. **2009**, 131, 1352–1353.
- (38) Ohnuma, A.; Cho, E. C.; Jiang, M.; Ohtani, B.; Xia, Y. *Langmuir* **2009**, *25*, 13880–13887.
- (39) Popp, P. S.; Herrmann, J. F.; Fritz, E. C.; Ravoo, B. J.; Höppener, C. Small **2016**, *12*, 1667–1675.